PAPER

CrossMark
← click for updates

Spatial distribution and temporal evolution of DRONPA-fused SNAP25 clusters in adrenal chromaffin cells†

Yasuko Antoku,[a] Peter Dedecker,[b] Paulo S. Pinheiro,[a] Tom Vosch*[c] and Jakob Balslev Sørensen*[a]

Sub-diffraction imaging of plasma membrane localized proteins, such as the SNARE (*Soluble NSF Attachment Protein Receptor*) proteins involved in exocytosis, in fixed cells have resulted in images with high spatial resolution, at the expense of dynamical information. Here, we have imaged localized fluorescence bursts of DRONPA-fused SNAP-25 molecules in live chromaffin cells by Total Internal Reflection Fluorescence (TIRF) imaging. We find that this method allows tracking protein cluster dynamics over relatively long times (~20 min.), partly due to the diffusion into the TIRF field of fresh molecules, making possible the simultaneous identification of cluster size, location and temporal evolution. The results indicate that the DRONPA-fused SNAP-25 clusters display rich dynamics, going from staying constant to disappearing and reappearing in specific cluster domains within minutes.

Introduction

SNARE proteins constitute a family of proteins which assemble a complex between vesicles and the plasma membrane to allow vesicle-to-membrane fusion (exocytosis) and the release of vesicular content.[1,2] SNAREs are expressed at high levels in neurons and neurosecretory cells, although the assembly of one to three complexes appears to be enough to drive fusion of a vesicle.[3] Most plasma membrane (target-) SNAREs are present in cholesterol-dependent clusters on the plasma membrane, from which they probably have to be recruited to function in exocytosis.[4] These clusters have been widely studied using superresolution microscopy, both because of their assumed importance in exocytosis, and because they served early on as an example for the power of such methods.

[a]*Department of Neuroscience and Pharmacology and Center for Biomembranes in Nanomedicine (CBN), University of Copenhagen, Blegdamsvej 3, 2200 Copenhagen, Denmark. E-mail: jakobbs@sund.ku.dk*
[b]*Department of Chemistry and Institute for Nanoscale Physics and Chemistry, Katholieke Universiteit Leuven, Celestijnenlaan 200F, 3001 Heverlee, Belgium*
[c]*Nano-Science Center/Department of Chemistry, University of Copenhagen, Universitetsparken 5, 2100 Copenhagen, Denmark. E-mail: tom@chem.ku.dk*

†Electronic supplementary information (ESI) available: Rescue data for the DRONPA_SNAP-25 construct. An example of a 2D Gaussian fit of a single molecule and an example of the localization accuracy. Two examples of a SRIC images. Average intensity image and second order SOFI image. Additional L(r)-r functions of live and fixed Chromaffin cells. Data on the effect of 405 nm light on the number of detected single molecules. Additional traces from live and fixed Chromaffin cells showing cluster dynamics. See DOI: 10.1039/c4pp00423j

Most investigations of the subdiffraction localization of SNAREs have utilized fixed cells combined with antibody-staining. This technique yields very high spatial resolution, because the fixation together with the use of bright chemical dyes allows for accurate localization of individual fluorophores. These investigations have resulted in the detailed description of sizes and numbers of SNARE-clusters in secretory cells. In PC12-cells, syntaxin-1 clusters are 50–100 nm in diameter, and have a density of 13–20 clusters μm^{-2},[2,5,6] whereas SNAP-25 clusters appears to be a bit larger, ~130 nm in diameter, and have a density of ~10 clusters μm^{-2}.[2,6] The two cluster types only partially overlap.[7,8] This method has also resulted in the identification of single SNAREs outside clusters, and numerical simulations have been used to suggest that clusters and individual molecules might be in a dynamic equilibrium.[5,6] However, in those experiments, which used fixed cells, these supposed dynamics could not be directly observed.

Another approach has been to track individual SNARE molecules tagged by fluorescent proteins (for instance Enhanced Green Fluorescent Protein, EGFP) over time in live cells. To allow resolution of single molecules, this was combined with low expression levels.[9,10] The results showed capture of SNAREs beneath secretory vesicles, indicating that the clustering dynamics is affected – or maybe even induced – by the secretory vesicles themselves.[9,10] However, using very low expression levels of tagged protein in cells expressing endogenous (non-tagged) SNAREs at high levels, a picture of the entire functional SNARE population is not obtained. In contrast, when visualizing the entire SNARE pool it was

reported that secretory vesicles dock in areas with low t-SNARE density.[11]

Here, we attempted to image the entire functional SNAP-25 population and study the temporal dynamics of the protein clusters, by visualising DRONPA-fused SNAP-25 (DRONPA_S-NAP25) expressed in live *Snap-25* null cells. This approach represents a compromise between the two strategies mentioned above, offering the ability to localize fluorescence bursts from DRONPA_SNAP25 constructs within a short time frame and dynamics of clusters over longer time frames. This makes it possible to address the dynamics of the clusters themselves at higher SNAP-25 expression levels. Our experiments show that some SNAP-25 clusters are stable over the course of ~10 min, while other clusters dissolve and form dynamically within minutes – sometimes several times. This verifies that SNARE-clusters are dynamic entities, and that fusion constructs between SNARE proteins and photoswitchable fluorophores can be used for studying cluster dynamics while retaining physiological functionality.

Material and methods

Chromaffin cell preparation and viral expression system

Snap-25 null embryos were obtained by crossing heterozygotes and performing caesarean section at E17–E18. Preparation of adrenal glands and cultivation of chromaffin cells were performed as described before.[12] Plasmids needed for the production of Semliki Forest viruses (SFV) were generated by standard molecular biology techniques. The SNAP-25 and DRONPA fragments were generated from plasmids encoding SNAP-25A[13] and DRONPA (the latter was a kind gift of Dr Atsushi Miyawaki).[14] A SNAP-25A fragment generated by PCR primer extension was cloned in between the unique ClaI and BssHII sites in a modified pSFV1 plasmid containing a multiple cloning site. Subsequently, a DRONPA fragment generated by PCR and lacking a stop codon was cloned into the plasmid in frame with SNAP-25A using upstream restriction sites BamHI and ClaI and resulting in N-terminal fusion of DRONPA to SNAP-25A *via* a 7 amino acid linker (referred to as DRONPA_SNAP-25). The construct was verified by sequencing before production of SFV particles using published protocols.[15] For experiments, stored virus aliquots were activated by chymotrypsin cleavage, followed by inactivation with aprotinin, and chromaffin cells were infected at days 2–4 after isolation. Images were recorded at room temperature 6–8.5 h after infection of SNAP-25 null adrenal chromaffin cells with viruses. Functional activity of the DRONPA_SNAP-25 construct was demonstrated after expression of DRONPA_SNAP-25 in *Snap-25* null cells. Secretion was evaluated by calcium uncaging, capacitance measurements and amperometry, as previously described.[12]

Total internal reflection fluorescence (TIRF) microscopy

Fluorescence imaging was performed on an inverted Ti-E Nikon Microscope using an Apochromat TIRF 100× 1.49NA oil immersion objective (Nikon). Chromaffin cells were placed on a poly-D-Lysine coated Chamber Coverglass (Sigma-Aldrich, Nunc® Lab-Tek® II Chambered Coverglass). Chromaffin cells were imaged in extracellular solution at room temperature. The composition of the extracellular solution was (in mM): 145 NaCl, 2.8 KCl, 2 CaCl$_2$, 1 MgCl$_2$, 10 HEPES and 11 glucose, pH 7.2 (osmolarity was adjusted to approximately 300 mOsm). For the fixed cell samples, the chromaffin cells were washed three times using phosphate buffered saline (PBS), prewarmed to 37 °C, fixed with 4% paraformaldehyde for 20 min at room temperature, and finally washed three times in PBS before being subjected to the imaging. The cells expressing photoswitchable DRONPA fused N-terminally to SNAP-25 (DRONPA_SNAP25) were excited by 488 nm laser light under TIRF illumination. The 488 nm excitation power was varied in some experiments and is expressed throughout in units of A.U., for which 100 A.U. corresponds to 7.3 mW in wide field configuration on the microscope. Intensity changes during the experiment were estimated from the relative background level changes of excitation light bleed-through and Raman in regions where no cells were present. For experiments where a 405 nm laser was used, 100 A.U. correspond to 200 µW in wide field configuration on the microscope. Fluorescence images were taken with an EMCCD camera (Ixon DU897, Andor) using a dichroic mirror (Z405/488rpz dichroic, Chroma) and emission filters (ET525/50m, Chroma and 488 nm RazorEdge ultra-steep long-pass edge filter, Semrock), resulting in an image pixel size of 160 nm. Images were acquired with an EM gain of 400–600 at 20 Hz. Data analysis, including localization of fluorescence bursts, drift correction and cluster analysis using Ripley's function,[16] was performed using the open source software Localizer.[17] Settings used in the Localizer software were; localization algorithm: Gaussian, particle finding: 8-way adjacency, GLRT insensitivity: 28, standard deviation of the point spread function in pixels: 1.6. The L(r)-r function was used to estimate the cluster radius *R*, where the maximum value of the L(r)-r function gives a value between *R* and 2*R*, depending on the intercluster separation.[16] It is a measure that compares the observed distances between the fitted spots with the distances that would be expected for truly randomly positioned (*i.e.* non-interacting) spots. Positive values indicate a preference to cluster together, negative values indicate the opposite. A value of zero suggests a random distribution. Drift correction of the localization data was performed on the basis of subimage registration. Briefly, for every movie we divided the fitted positions into different groups. These groups were chosen such that the spots fitted at the very beginning of the experiment went into the first group, spots fitted a short time later went into the second group, and so on. Typically each group contained approximately 10 000 spots. We then used these 10 000 spots to generate localization images. By comparing the shift between consecutive images using correlation analysis, we obtained estimates for the drift displacement, and used these to correct for this drift. For the SOFI analysis, we additionally used these estimates to generate a drift-corrected dataset where each camera image was shifted by the corresponding drift using interpolation.

Results and discussion

TIRF microscopy of DRONPA_SNAP25 in live chromaffin cells

To be able to visualize the entire functional SNAP-25 pool, we expressed DRONPA_SNAP25 in chromaffin cells from *Snap-25* null mice. This fusion construct was fully functional, as demonstrated by rescue of calcium-stimulated exocytosis upon expression (Fig. SI1†). Our use of DRONPA as the fluorophore was motivated by this protein's reversible photochromism, in which DRONPA molecules can cycle between a fluorescent and non-fluorescent state.[18,19] The continuous fluorescence fluctuations caused by DRONPA can be used to localize regions with high SNARE density with subpixel precision. The relatively high number of molecules of DRONPA active at any given time allows a favorable temporal resolution of clusters, but at the same time makes it hard to ensure that all spatially resolved observations represent individual fluorophores. Therefore, we prefer to refer to 'bright spots' instead of 'individual molecules'. Our approach therefore differs from diffraction-unlimited localization microscopy. The live chromaffin cells were seeded on a glass coverslip and the DRONPA_SNAP25 constructs in the membrane were visualized using 488 nm excitation in a total internal reflection (TIRF) configuration. Movies were recorded and the diffraction-limited fluorescence spots in the individual frames were fitted with a 2D Gaussian function using the software program Localizer,[17] making use of this program's functionality to selectively recognize diffraction-limited spots in the individual fluorescence images. The fitting allowed the determination of the central position of the 2D Gaussian (See Fig. SI2A† for an example) and hence locate the position of the bright spots (which does not necessarily represents the physical location of a single molecule) with an average accuracy of approximately 60 nm (See Fig. SI2B†). Fig. 1 shows two single frames of a movie of a live (Fig. 1A) and a fixed (Fig. 1B) chromaffin cell, which were analyzed using the Localizer software. In these particular frames, 11 and 12 single spots, respectively, met the predetermined requirement to be identified as highly localized bursts of fluorescence. These requirements include sufficient brightness and a local emission distribution sufficiently close to Gaussian, as seen in Fig. 1. We also observed some sample drift over the full length of the movie (30 000 images), which we corrected using the built-in Localizer functionality. As can be seen in Fig. 1A and B, a significant fluorescence signal is present between the localized fluorescence spots, which could be due to either mobile DRONPA_SNAP25 molecules or background fluorescence, or simply because insufficient emission was collected in that particular image and region to register as a localized fluorescence spot. The resulting list of *XY*-coordinates of the fluorescence bursts can be directly visualized (Fig. 2) and shows the spatial distribution of the localized bright DRONPA_SNAP25 signals.

Besides creating images displaying the positions of the individual DRONPA_SNAP25 constructs, the positions were binned into a new grid of 1300 by 1300 pixels where each pixel had a dimension of approximately 31 nm. As a result of the
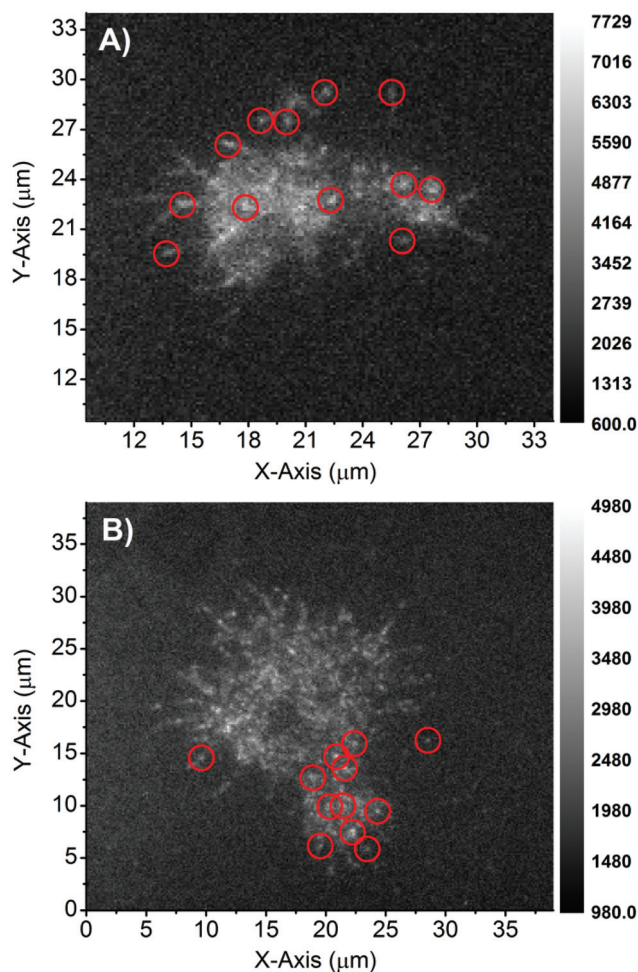

Fig. 1 Two examples of a single frame (50 ms integration time per frame, 488 nm excitation from a movie, showing a live (A) and a fixed (B) adrenal chromaffin cell that expressed the DRONPA_SNAP25 constructs. The red circles shows the detected fluorescence bursts, indicating zones of highly localized fluorescence. The scale bar on the right depicts the fluorescence intensity (A.U.).

binning, the intensity of each pixel represents the number of detected bright spots and represents the locations where more DRONPA_SNAP25 molecules are expected to be localized.[20] The result of such a reconstructed image, representing the positions of all detected bright spots in a movie of 30 000 frames, can be seen in Fig. 2B. The intensity scale represents the number of fluorescence bursts per pixel. In certain areas, clusters with a high number of bursts are present, while in other areas virtually no bursts were detected. Four such cluster regions are indicated with small colored boxes and will be investigated in more detail below. We are of course bound by experimental conditions and one cannot exclude that the photophysics of DRONPA could be localization dependent[21] in living cells or that the cell membrane is not firmly attached everywhere on the cover slip, in spite of being attached through poly-lysine. Regarding the latter point, we have added two representative Surface Reflective Interference Contrast
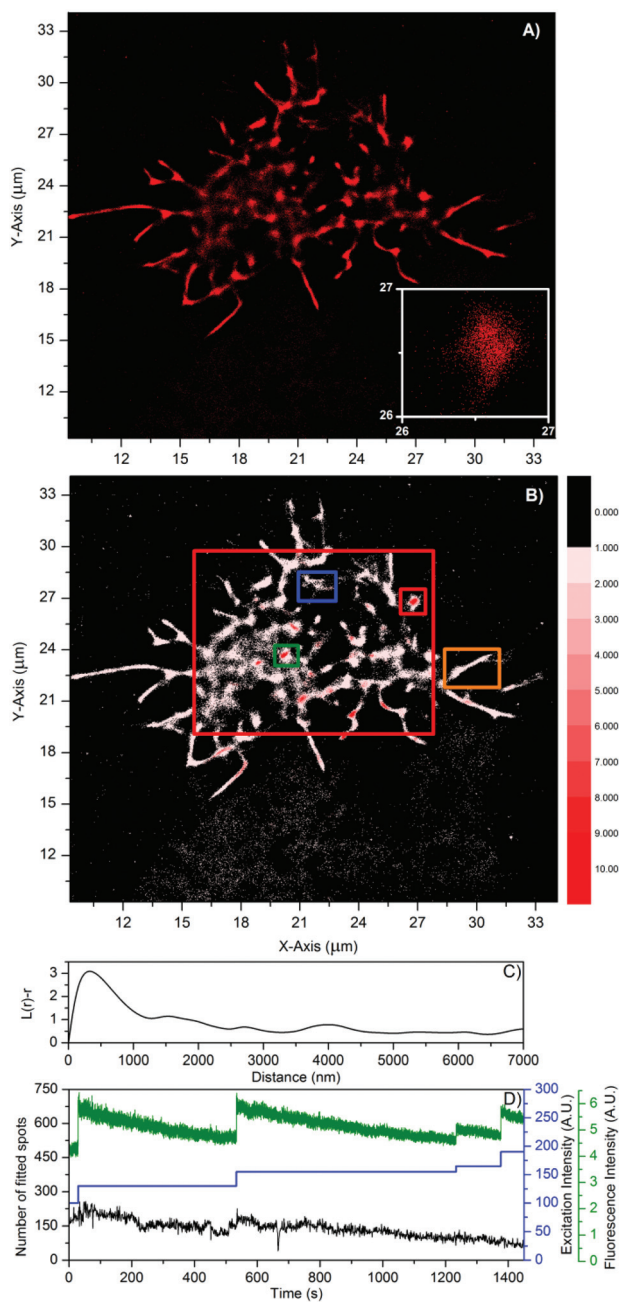
This journal is © The Royal Society of Chemistry and Owner Societies 2015

Photochem. Photobiol. Sci., 2015, **14**, 1005–1012 | **1007**

Fig. 2 Reconstructed images displaying all the DRONPA_SNAP25 related bright spots in a movie of 30 000 frames (approximately 1450 seconds) from a live chromaffin cell (a single frame of the original movie can be seen in Fig. 1) for which the center of its position was determined by the Localizer software. (A) Is an image where the center of each bright spot is represented as a red dot while (B) is an image where the dots are rebinned in a grid with a pixel size of 32 by 32 nm. The intensity scale represents the number of bright spots per pixel. (C) L(r)-r function of the area in (B) indicated with the large red box. (D) Time evolution of the number of bright spots (black curve and black Y-axis), the 488 nm excitation power and the total fluorescence intensity (green curve and green Y-axis) in the recorded movie.

(SRIC) images of similar living Chromaffin cells attached in the same way as the cells shown in the paper (See Fig. SI3†). These images indicate that at least some of the dark regions

can be related to not full attachment of the membrane to the coverslip. Additionally, a diffraction limited, drift corrected average intensity image of the first 20 000 frames of the movie used to create Fig. 2 can be seen in Fig. SI4A.† Similar brighter regions (clusters) can be observed, but by fitting only the bright bursts, we can suppress the diffuse fluorescence background (due to fast lateral diffusing DRONPA_SNAP25 or auto fluorescence).

We assumed that the spatial organization of the emission bursts provided insight into the spatial distribution of the DRONPA_SNAP25 molecules. We subjected the detected (x, y) coordinates of these bursts to a cluster analysis to gain information on the length scale at which the DRONPA_SNAP25 distribution is organized. An L(r)-r function was used,[16] which estimates the cluster radius R, where the maximum value of the L(r)-r function gives a value between R and $2R$, depending on the intercluster separation.[16] The area used to calculate the L(r)-r function is indicated in Fig. 2B with a large red box and the resulting L(r)-r is given in Fig. 2C. Based on this L(r)-r function, a first prominent feature (maximum in the L(r)-r function) can be observed around 300 nm.[6] Fig. SI5† shows the L(r)-r functions of 5 different live and fixed cells which all show a similar first maximum in the function appearing between 250 nm and 500 nm. Fig. 2D shows the temporal evolution of the number of detected bright spots (black curve). The number of detected bright spots starts around 200 at the beginning of the experiment (1 second bin) and drops to about 100, after 1450 seconds, at the end of the experiment. Interestingly, only 488 nm excitation light was used to excite DRONPA and despite the fact that 488 nm light is known to photoconvert DRONPA molecules to a dark state,[14] the number of bright spots only dropped by a factor of 2 over the course of the whole experiment (1450 seconds). The green curve in Fig. 2D represents the total fluorescence intensity in the whole frame as a function of time and the blue curve represents the 488 nm excitation intensity changes. As can be seen in Fig. 2D, at four points during the experiment, the excitation intensity of the 488 nm laser was increased. This leads to an increase of the total overall fluorescence in the green curve. The number of detected bright spots is not markedly affected when the 488 nm excitation power was increased in this case. However, due to the fitting criteria, it is sometimes possible for certain movies to see a correlation between increasing the 488 nm excitation intensity and the number of detected bright spots. This is due to the fact that increasing the excitation intensity might change the signal (DRONPA_SNAP25 fluorescence)-to-background ratio in such a way that more or less spots will be considered as a valid detection event. However, for the data from the movie presented in Fig. 2, this was not the case in a significant way. As an additional check, we also performed a SOFI (super-resolution optical fluctuation imaging)[19,22] analysis of the same movie presented in Fig. 2 (see Fig. SI4B†). Fig. SI4B† clearly shows similar cluster features which strengthens the value of the approach we propose here. The overall gradual drop in the number of bright spots in Fig. 2 could be explained by two

1008 | Photochem. Photobiol. Sci., 2015, 14, 1005–1012

This journal is © The Royal Society of Chemistry and Owner Societies 2015

possible mechanisms. One mechanism could be that DRONPA_SNAP25 molecules continuously move into the imaged membrane regions and another mechanism is that the switched off DRONPA molecules switch back to the emissive state.[18,19] If one of those two mechanisms were rate limiting, it would also explain why the number of detected bright spots does not drop when increasing the 488 nm excitation.

To test whether there is a significant number of dark DRONPA_SNAP25 molecules present in the membranes due to continuous excitation with the 488 nm laser, an experiment was performed where 405 nm light was switched on during the experiments, keeping the 488 nm constant. The results can be seen in Fig. SI6.† Switching on the 405 nm laser and increasing its intensity leads to a correlated jump in the number of detected bright spots both for the overall image of the whole live chromaffin cell (black curve in Fig. SI6B†) and for a selected cluster domain (Fig. SI6C,† see Fig. SI6A red box for the area analyzed). However, after the initial increase of the number of bright spots upon increasing the 405 nm excitation intensity, the number steadily decreases again to the same level as before the excitation intensity increase. The latter is surprising since one would expect that photo activation with 405 nm would lead to a higher, but fairly constant number of DRONPA_SNAP25 related bright spots since usually DRONPA can switch many times back and forth between the dark and bright state.[18] However, this observation is in line with the suggestion above, that the number of emissive molecules is not limited by photo activation, but either by diffusion or spontaneous switching back to the emissive state.

In order to investigate the local dynamics of individual DRONPA_SNAP25 cluster regions, the original movie of 30 000 frames was split up into 6 fragments of 5000 frames each. Fig. 3 shows the spatial distribution of the detected bright spots in each of the subset of 5000 frames. What is clearly observable is that the amount of detected bright spots in a specific area changes over time. In certain areas the clusters can completely disappear while in other areas clusters appear where none where present in the previous image. In order to evaluate the evolution of the characteristic cluster domain size over time, L(r)-r functions for each of the subsets were constructed and the results can be seen in Fig. 4A. The six L(r)-r functions in Fig. 4A show a first feature around 300 nm. It is clear from Fig. 4A that despite the visual changes in the distribution of the bright spots in the six images in Fig. 3, the first feature with a radius around 300 nm stays practically constant throughout the 6 images. Only some fluctuations in the features larger than 1000 nm can be observed. The time evolution of the L(r)-r functions seem to suggest that despite the visual changes of the distribution of bright spots that can be observed in the images in Fig. 3, a typical maximum around 300 nm (corresponding to a real radius between 150 and 300 nm) is present at all times.

In order to illustrate the temporal evolution of clusters in more detail, the number of detected spots was plotted as a function of time for 4 selected domains, indicated in Fig. 2B
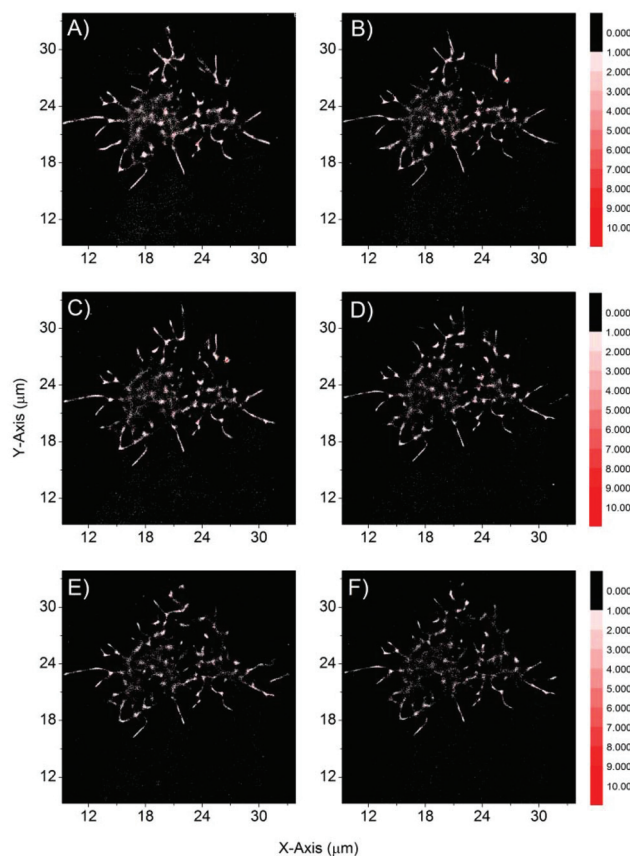

Fig. 3 Temporal evolution of the reconstructed image from DRONPA_SNAP25 related bright spots in a live chromaffin cell using the Localizer program. The six images are created from subsets of the total movie (data from the same movie as Fig. 1 and 2). (A) 1–5000 frames, (B) 5001–10 000 frames, (C) 10 001–15 000 frames, (D) 15 001–20 000 frames, (E) 20 001–25 000 frames, (F) 25 001–30 000 frames. Each frame had an integration time of 50 ms.

with small red, blue, green and orange boxes. The red and blue boxes are examples of regions where large variations in the number of detected bright spots over time (the cluster completely disappears and then reappears), while the green and orange box are examples of regions where the number of detected bright spots stayed fairly constant over time. ESI† section 4A shows a total of 48 DRONPA_SNAP25 cluster regions that were tracked over time for 5 different live cells. The traces display similar behavior to the 4 examples presented in Fig. 4. It is hard to quantify the rich dynamics that is observed in these traces; however they are clearly different from the DRONPA_SNAP25 cluster traces in ESI† section 4B obtained from fixed cells which show a gradual, exponential-like drop, in the number of detected bright spots over time (see below).

For the two domains indicated with the small red and blue boxes in Fig. 2B, for which the temporal evolution can be seen in Fig. 4B and C, a map was constructed showing the spatial distribution of where the individual bright spots were detected in the six subsets (Fig. 5). Both clusters showed large fluctu-
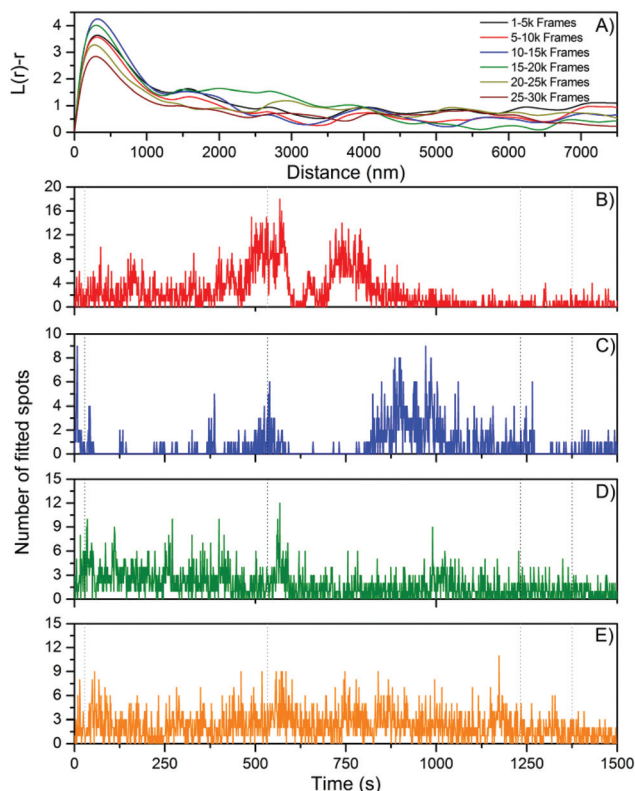
This journal is © The Royal Society of Chemistry and Owner Societies 2015

Photochem. Photobiol. Sci., 2015, 14, 1005–1012 | 1009

Fig. 4 (A) Evolution of the L(r)-r function of the live chromaffin cell displayed in Fig. 2 (area used to calculate L(r)-r function is shown as the large red box in Fig. 2B. The color represents on which subset of the total movie the L(r)-r function was calculated. The black curve is from the first 5000 frames, red from 5001 to 10 000 frames, blue from 10 001 to 15 000 frames, green from 15 001 to 20 000 frames, dark yellow from 20 001 to 25 000 frames, brown from 25 001 to 30 000 frames. (B–E) Temporal evolution of the number of fitted spots for specific cluster domains. B is from the area in Fig. 2B represented by the small red box, C the blue box, D the green box and E the orange box. The gray dotted lines represent points when the 488 nm excitation power was increased.

Fig. 5 Temporal evolution of the positional distribution of DRONPA_S-NAP25 related bright spots for (A) the cluster domain represented in Fig. 4B and (B) the cluster domain represented in Fig. 4C. The spots are color coded, representing in which subset of the movie they were observed. Black is from the first 5000 frames, red from 5001 to 10 000 frames, blue from 10 001 to 15 000 frames, green from 15 001 to 20 000 frames, dark yellow from 20 001 to 25 000 frames, brown from 25 001 to 30 000 frames.

ations in the number of detected bright spots over time and the cluster even disappeared at some point. However, the positions where the bright spots are detected for the domain in Fig. 4B seem to change as a function of time (Fig. 5A), while for the domain in Fig. 4C it seems to stay more or less at the same position throughout the experiment (Fig. 5B).

TIRF microscopy of DRONPA_SNAP25 in fixed chromaffin cells

In order to validate the observed DRONPA_SNAP25 cluster dynamics observed in live chromaffin cells, the experiments were repeated with fixed chromaffin cells. The latter will obviously prevent diffusion or active transport of new DRONPA_SNAP25 molecules. Fig. 6A shows an image reconstructed with the detected bright spots in a fixed chromaffin cell. Fig. 6B shows the L(r)-r function of the large red box represented in Fig. 6A. The L(r)-r function shows a similar first feature around 300 nm as for the live chromaffin
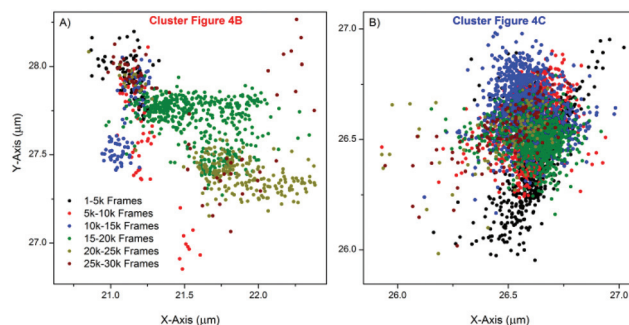
case. However, the most dramatic difference between the live and the fixed cells is when we follow as a function of time the number of detected bright spots throughout the whole fixed cell or in an individual domain. Compared to the live cell case, the number of detected bright spots decayed rapidly in a gradual, exponential-like fashion as can be seen in the black curve in Fig. 6C. A similar observation on DRONPA in fixed HeLa cells was made by Mizuno *et al.*[23]

This exponential-like fashion could be due to photobleaching or photoconversion and one cannot rule out that the fixation altered the photobleaching and spontaneous back switching from the dark state. Although this faster disappearance of DRONPA limits the collection time window, it is still long enough for determining the cluster size found in a living and fixed cell and similar clusters sizes (first maximum in the L(r)-r function) were found as can be seen in Fig. SI5.† The overall fluorescence (green curve) shows the same trend and the excitation power of the 488 nm laser was kept constant in this experiment (blue curve). Switching on the 405 nm UV laser in the second half of the experiment and increasing its excitation intensity, led to an increase in the number of detected bright spots and overall fluorescence, which was followed again by a decrease as a function of time (See Fig. 6C). This response from DRONPA upon irradiation with 405 nm light is similar as observed for the live chromaffin cell case (See Fig. SI6†), indicating that at least some photoactivated back switching from the dark state is still possible. A similar exponential drop in the number of detected bright spots was also found for single domains. A temporal evolution in the number of detected bright spots for the small red and blue box in Fig. 6A can be seen in Fig. 7A and B. A similar exponential-like decay is observed and, in contrast to live chromaffin cells, no oscillatory dynamics can be observed that are not correlated to changes in the excitation power of either 488 nm or 405 nm.
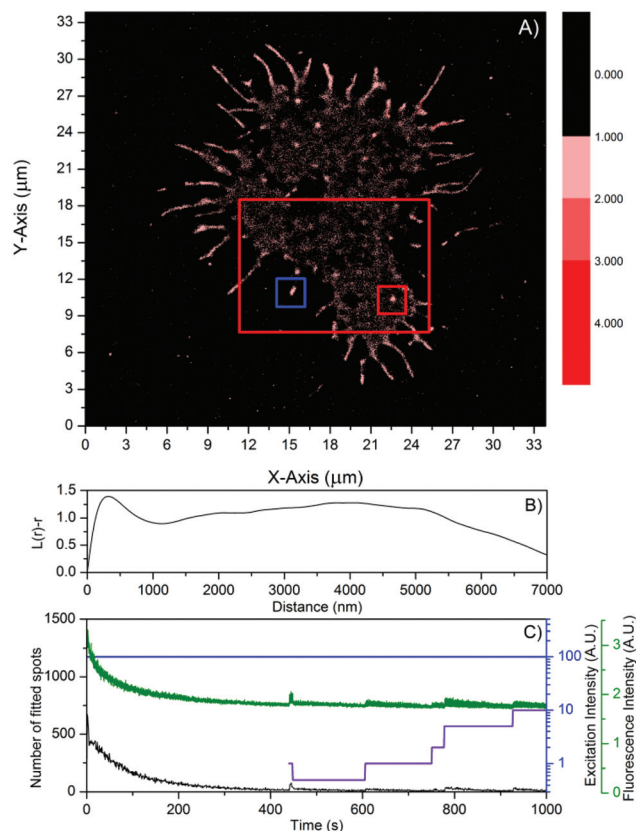
Fig. 6 (A) Reconstructed image displaying all the bright spots in a movie of 12 578 frames (approximately 1000 seconds) from a fixed chromaffin cell for which the center of its position was determined by the Localizer software. (B) L(r)-r function of the area in (A) indicated with the large red box. (C) Temporal evolution of the number of detected and fitted bright spots (black curve and black Y-axis), the 488 nm excitation power (blue curve and blue Y-axis), 405 nm excitation power (purple curve and blue Y-axis) (the A.U. for the 488 nm and the 405 nm are not the same) and the total fluorescence intensity (green curve and green Y-axis) in the recorded movie.
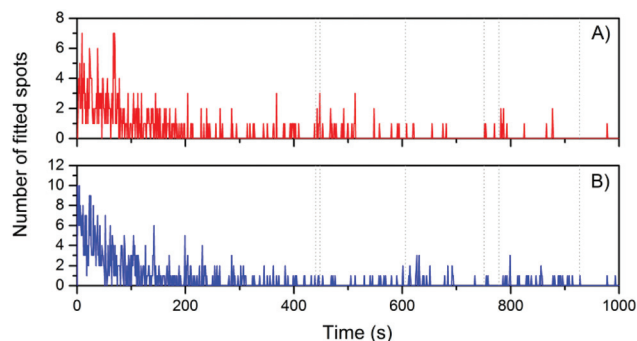

Fig. 7 Temporal evolution of the number of detected bright spots for specific cluster domains in a fixed chromaffin cell. (A) is from the area in Fig. 6A represented by the small red box and (B) the blue box. The gray dotted lines represents points when the 405 nm excitation power was changed (see also Fig. 6).

Conclusions

Using TIRF microscopy we obtained positional information on DRONPA_SNAP25 clusters in live and fixed chromaffin cells. With 488 nm excitation and TIRF illumination, the Localizer software allowed visualizing the dynamics of the number of DRONPA_SNAP25 related bright spots in clustered domains. As explained in the Introduction, this approach represents a compromise between determining the spatial localization of single molecules and being able to follow the dynamics of clusters in biologically relevant conditions. Also, we were able to identify overall clustering and approximate cluster sizes (using the L(r)-r function) and follow the evolution of clusters domains. A few observations are worthy of note:

1. Imaging of live cells happened on a larger background of diffuse fluorescence than in fixed cells. One hypothesis is rapid diffusion of single molecules beyond our temporal detection limit. Diffuse fluorescence of EGFP fused to SNAP25 was previously noted to be more prominent than for syntaxin constructs, probably both because of faster diffusion of SNAP-25, and because its expression level is higher.[10] To image single SNAP-25 molecules as such, brighter dyes or faster acquisition times are required, together with approaches to overcome the concentration barrier. However, with genetically encoded dyes it is probably unavoidable that many diffusing molecules add to the background. Note that this is also a function of expression level; at much lower expression levels single molecules might be tracked, but at high expression levels this will be very difficult or impossible.

2. DRONPA-SNAP25 could be visualized over long times in live cells using only 488 nm excitation without, or after brief initial, 405 nm activation. In contrast, in fixed cells a gradual, exponential-like disappearance was present as a function of time. The latter was most likely due to photobleaching or photoconversion into a dark state. One can not exclude that the photophysics of DRONPA is affected by the fixation. Another likely reason for the different observations in live and fixed cells is that diffusion of single activated molecules into the TIRF-field – or spontaneous back switching to the emissive state – is fast enough in live cells to partially compensate for the fluorophores that are lost.

3. As a result of lateral diffusion limiting resolution, the imaging of DRONPA-SNAP25 produces a picture biased towards those molecules which arrest their movement for long enough to be captured. In this way the method is geared towards detecting clusters where molecules remain relatively stationary. Together with the continuous supply of new DRONPA-molecules, this makes it possible to image these clusters, and their dynamics, over relatively long times (10–30 min.).

Our results from the live chromaffin cells showed rich dynamics of DRONPA-SNAP25 clusters, going from staying constant to disappearing and reappearing of molecules in specific cluster domains. Spontaneous formation and disappearance was demonstrated for EGFP-syntaxin in live PC-12 cells,[9] whereas syntaxin clusters in 'unroofed' cells were

This journal is © The Royal Society of Chemistry and Owner Societies 2015

Photochem. Photobiol. Sci., 2015, **14**, 1005–1012 | **1011**

reported to be stationary.[5] Our data extend these finding to show that clusters of SNAP-25 in live cells at high expression levels are dynamic entities, with characteristic times for generation/disappearance in the range of minutes. We also observed in some cases lateral movement of the clusters themselves, indicating that dynamics might take place on more than one scale. The presented data shows that fluorescence localization microscopy and the Localizer software can be used to track the dynamics of clusters of fluorescently labeled proteins over time in living cells.

Acknowledgements

Notes and references

1 R. Jahn and D. Fasshauer, *Nature*, 2012, **490**, 201–207.
2 T. C. Sudhof and J. E. Rothman, *Science*, 2009, **323**, 474–477.
3 R. Mohrmann and J. B. Sorensen, *J. Mol. Neurosci.*, 2012, **48**, 387–394.
4 G. van den Bogaart, T. Lang and R. Jahn, *Curr. top. membr.*, 2013, **72**, 193–230.
5 J. J. Sieber, K. I. Willig, C. Kutzner, C. Gerding-Reimers, B. Harke, G. Donnert, B. Rammner, C. Eggeling, S. W. Hell, H. Grubmuller and T. Lang, *Science*, 2007, **317**, 1072–1076.
6 D. Bar-On, S. Wolter, S. van de Linde, M. Heilemann, G. Nudelman, E. Nachliel, M. Gutman, M. Sauer and U. Ashery, *J. Biol. Chem.*, 2012, **287**, 27158–27167.
7 M. Ohara-Imaizumi, C. Nishiwaki, Y. Nakamichi, T. Kikuta, S. Nagai and S. Nagamatsu, *Diabetologia*, 2004, **47**, 2200–2207.
8 T. Lang, D. Bruns, D. Wenzel, D. Riedel, P. Holroyd, C. Thiele and R. Jahn, *EMBO J.*, 2001, **20**, 2202–2213.
9 S. Barg, M. K. Knowles, X. Chen, M. Midorikawa and W. Almers, *Proc. Natl. Acad. Sci. U. S. A.*, 2010, **107**, 20804–20809.
10 M. K. Knowles, S. Barg, L. Wan, M. Midorikawa, X. Chen and W. Almers, *Proc. Natl. Acad. Sci. U. S. A.*, 2010, **107**, 20810–20815.
11 L. Yang, A. R. Dun, K. J. Martin, Z. Qiu, A. Dunn, G. J. Lord, W. Lu, R. R. Duncan and C. Rickman, *PLoS One*, 2012, **7**, e49514.
12 J. B. Sorensen, G. Nagy, F. Varoqueaux, R. B. Nehring, N. Brose, M. C. Wilson and E. Neher, *Cell*, 2003, **114**, 75–86.
13 I. Delgado-Martinez, R. B. Nehring and J. B. Sorensen, *J. Neurosci.*, 2007, **27**, 9380–9391.
14 R. Ando, H. Mizuno and A. Miyawaki, *Science*, 2004, **306**, 1370–1373.
15 U. Ashery, A. Betz, T. Xu, N. Brose and J. Rettig, *Eur. J. Cell Biol.*, 1999, **78**, 525–532.
16 M. A. Kiskowski, J. F. Hancock and A. K. Kenworthy, *Biophys. J.*, 2009, **97**, 1095–1103.
17 P. Dedecker, S. Duwe, R. K. Neely and J. Zhang, *J. Biomed. Opt.*, 2012, **17**, 126008.
18 S. Habuchi, R. Ando, P. Dedecker, W. Verheijen, H. Mizuno, A. Miyawaki and J. Hofkens, *Proc. Natl. Acad. Sci. U. S. A.*, 2005, **102**, 9511–9516.
19 P. Dedecker, G. C. H. Mo, T. Dertinger and J. Zhang, *Proc. Natl. Acad. Sci. U. S. A.*, 2012, **109**, 10909–10914.
20 M. B. J. Roeffaers, G. De Cremer, J. Libeert, R. Ameloot, P. Dedecker, A. J. Bons, M. Buckins, J. A. Martens, B. F. Sels, D. E. De Vos and J. Hofkens, *Angew. Chem., Int. Ed.*, 2009, **48**, 9285–9289.
21 Y.-T. Kao, X. Zhu and W. Min, *Proc. Natl. Acad. Sci. U. S. A.*, 2012, **109**, 3220–3225.
22 T. Dertinger, R. Colyer, R. Vogel, J. Enderlein and S. Weiss, *Opt. Express*, 2010, **18**, 18875–18885.
23 H. Mizuno, P. Dedecker, R. Ando, T. Fukano, J. Hofkens and A. Miyawaki, *Photochem. Photobiol. Sci.*, 2010, **9**, 239–248.